



Article

Genome-Wide Identification of the *DGK* Gene Family in Kiwifruit (*Actinidia valvata* Dunn) and an Expression Analysis of Their Responses to Waterlogging Stress

Meijuan Zhang^{1,2}, Cuixia Liu^{1,*}, Faming Wang¹, Shibiao Liu³, Jianyou Gao¹, Jiewei Li¹, Quanhui Mo¹, Kaiyu Ye¹, Beibei Qi¹  and Hongjuan Gong¹

¹ Guangxi Key Laboratory of Plant Functional Phytochemicals and Sustainable Utilization, Guangxi Institute of Botany, Guangxi Zhuang Autonomous Region and Chinese Academy of Sciences, Guilin 541006, China; zmj521good@163.com (M.Z.); wfm@gxib.cn (F.W.); gjy@gxib.cn (J.G.); lijw@gxib.cn (J.L.); moqh@gxib.cn (Q.M.); yky@gxib.cn (K.Y.); qbb@gxib.cn (B.Q.); gongjian-3000@sohu.com (H.G.)

² College of Biology Pharmacy and Food Engineering, Shangluo University, Shangluo 726000, China

³ College of Biology and Environmental Sciences, Jishou University, Xiangxi 416000, China; liushibiao_1@163.com

* Correspondence: liucuixia@gxib.cn

Abstract: Diacylglycerol kinase (DGK) is a lipid kinase that phosphorylates diacylglycerol (DAG) to generate phosphatidic acid (PA). Based on converting one important signaling molecule (DAG) to another (PA), DGK plays an important role in plant responses to abiotic stress, including waterlogging stress. However, no studies have been reported on the characterization of the *DGK* gene family in the waterlogging-tolerant kiwifruit germplasm *Actinidia valvata* Dunn. In this study, we identified 18 *AvDGK* genes in the *A. valvata* genome. The phylogenetic analysis showed that *AvDGKs* can be classified into three clusters, and members within the same cluster have similar domain distributions, exon-intron structures, and conserved motif compositions. The chromosome localization analysis revealed that all *AvDGK* genes are located across 18 different chromosomes. There were 29 duplicated gene pairs in *A. valvata* and all had undergone purifying selection during evolution. The promoter *cis*-element analysis revealed that the *cis*-elements within *AvDGK* genes are associated with multiple functions, including phytohormone signal transduction, stress responses, and plant growth and development. The expression pattern analyses indicated that *AvDGKs* play important roles in fruit development and plant responses to waterlogging stress. The *AvDGK* gene family in the tetraploid *A. valvata* genome might promote PA synthesis and subsequent signal transduction both under short- and long-term waterlogging stresses. These results provide information regarding the structural characteristics and potential function of *AvDGK* genes within *A. valvata* and lay a fundamental basis for further research into breeding to enhance the kiwifruit's tolerance to waterlogging stress.

Keywords: *Actinidia valvata*; diacylglycerol kinase; expression pattern; phylogenetic analysis; waterlogging stress



Citation: Zhang, M.; Liu, C.; Wang, F.; Liu, S.; Gao, J.; Li, J.; Mo, Q.; Ye, K.; Qi, B.; Gong, H. Genome-Wide Identification of the *DGK* Gene Family in Kiwifruit (*Actinidia valvata* Dunn) and an Expression Analysis of Their Responses to Waterlogging Stress. *Horticulturae* **2024**, *10*, 310. <https://doi.org/10.3390/horticulturae10040310>

Academic Editors: Sara González-Orenga, M. Iftikhar Hussain and Muhammad Ikram

Received: 22 February 2024

Revised: 13 March 2024

Accepted: 19 March 2024

Published: 22 March 2024



Copyright: © 2024 by the authors. Licensee MDPI, Basel, Switzerland. This article is an open access article distributed under the terms and conditions of the Creative Commons Attribution (CC BY) license (<https://creativecommons.org/licenses/by/4.0/>).

1. Introduction

As the main structural components of cellular membranes, lipids also play a crucial role in cellular signal transduction. Among them, phosphatidic acid (PA) is an important signaling lipid molecule, and its cellular level fluctuates rapidly and transiently in response to various biotic and abiotic stresses [1–6]. The production of PA can be rapidly triggered in response to stimuli such as calcium [7,8], abscisic acid (ABA) [9], reactive oxygen species (ROS) [10], and other factors. As the simplest phospholipid, PA can be produced by hydrolyzing membrane phospholipids such as phosphatidylcholine (PC) by phospholipase D (PLD). Moreover, PA can also be synthesized by diacylglycerol kinase (DGK) by phosphorylating diacylglycerol (DAG), which is another main signaling molecule within eukaryotic

cells. Therefore, based on converting one important signaling molecule (DAG) to another (PA), DGKs play important roles in the regulation of plant growth, development, and adaptation to environmental stresses [11–14].

DGKs are a widespread family of enzymes in most multicellular organisms. Members of the DGK gene family have been identified in various plant species, including *Arabidopsis thaliana* (L.) Heynh. [14], *Oryza sativa* L. [15], *Phaseolus vulgaris* L. [16], *Brassica napus* L. [17], *Triticum aestivum* L. [18], *Malus domestica* (Suckow) Borkh. [19], *Glycine max* (L.) Merr. [20], *Zea mays* L. [21], and *Populus trichocarpa* (Torr. and Gray) [22]. In plants, DGKs are grouped into three phylogenetic clusters based on their domain structures and sequence similarities [13,14]. DGKs in all clusters possess a conserved catalytic domain featuring an ATP-binding site (consensus GXGXXG/A), which is essential for kinase activity [23]. Additionally, cluster I contains two C1-type domains, which are cysteine-rich domains thought to be responsible for binding the substrate DAG [24].

The roles of DGKs in different clusters also exhibit functional variations. In *Arabidopsis*, AtDGK1 in cluster I was expressed in the roots, leaves, and shoots but not in the flowers and siliques [12,25]. Conversely, the expression of AtDGK4 and AtDGK7 in cluster II was the strongest in flowers [26]. Similarly, OsDGK1 modulates the root architecture of rice by altering the density of lateral and seminal roots [27]. In *Arabidopsis*, the expression of AtDGK2 is transiently induced by wounding and cold stresses [23,26], while the expression of AtDGK5 (cluster III) increased under water and salt stresses [28]. Moreover, AtDGK5 is involved in regulating ROS production in plant immunity [2]. Furthermore, AtDGK1 and AtDGK5 were rapidly upregulated within 10 min after submergence, indicating that DGK may play a vital role in the short-term accumulation of PA under waterlogging stress [29].

Kiwifruit (*Actinidia* spp.) is widely favored for its high content of vitamin C, rich mineral elements, and delicious taste. Nevertheless, the quality and yield of kiwifruit are frequently affected by the negative impacts of waterlogging, as most of the kiwifruit cultivars possess fleshy roots that are susceptible to excess water [30,31]. *Actinidia*, a large genus comprising over 50 species, offers a great diversity of genetic resources for the development of new kiwifruit cultivars [32–34]. Notably, *A. valvata* is a shrub that mainly grows in Eastern China, and is commonly used as a rootstock in kiwifruit production due to its greater tolerance to waterlogging stress [35–37]. Several studies have been dedicated to clarifying the adaptive strategies employed by *A. valvata* for dealing with waterlogged conditions. It was reported that the waterlogging tolerance of *A. valvata* was associated with high activity levels of pyruvate decarboxylase (PDC), alcohol dehydrogenase (ADH) and antioxidant enzymes [35]. Additionally, *AvERF73* could improve the waterlogging tolerance by participating in the hypoxia response and mevalonate pathway [38]. However, the waterlogging tolerance mechanism of *A. valvata* rootstocks has not been well elucidated. Based on the important role of DGK in waterlogging stress, it is necessary to identify the DGK gene family in *A. valvata* and explore the role of *AvDGK* under waterlogging stress. In this study, we systematically identified and characterized the DGK family members in *A. valvata*. Additionally, we investigated the expression patterns of *AvDGKs* at different fruit development stages and under salt stress and their potential roles under waterlogging stress. Our findings provide information regarding the structural characteristics and potential function of DGK genes within kiwifruit and a fundamental basis for further breeding research aimed at enhancing the tolerance in kiwifruit under waterlogging stress.

2. Materials and Methods

2.1. Identification of DGK Genes in *A. valvata*

We used the *A. valvata* genome (unpublished, the leaf was sequenced by BGI Inc., Shenzhen, China) to identify and characterize the DGK genes. Two methods, blastp and hmmsearch, were employed to identify the DGK genes in kiwifruit. Seven DGK protein sequences of *A. thaliana* (AtDGK) were downloaded from the TAIR database (<https://www.arabidopsis.org/>) (accessed on 31 October 2023) [39] and used for the BLASTp analysis of the kiwifruit protein sequences. The DGK domains, including the diacylglycerol kinase catalytic domain (DAGK_cat/DAGKc/DGKc, PF00781) and diacylglycerol kinase accessory

domain (DAGK_acc/DAGKa/DGKa, PF00609), were retrieved from the Pfam database (<https://pfam.xfam.org/>) (accessed on 28 October 2023) [40]. These two domains were used to search the kiwifruit protein database using HMMER 3.0 (<https://www.ebi.ac.uk/Tools/hmmer/>) (accessed on 28 October 2023) [41]. The results of these two methods were merged and submitted to the NCBI-CDD website (<https://www.ncbi.nlm.nih.gov/cdd>) (accessed on 1 November 2023) and Pfam and SMART databases (<http://smart.embl-heidelberg.de/>) (accessed on 7 November 2023) to further confirm the DGK-conserved domains in each putative protein.

2.2. Physicochemical Properties, Protein Secondary Structure, and 3D Modeling of AvDGK Proteins

The physicochemical properties of the AvDGK proteins, such as the amino acid (A.A) length, molecular weight (M.W), and isoelectric point (pI), were evaluated using the ExPASy website (<https://www.expasy.org/>) (accessed on 31 October 2023). Cell-ploc 2.0 (<http://www.csbio.sjtu.edu.cn/bioinf/Cell-PLoc-2/>) (accessed on 7 November 2023) [42] was used to predict the subcellular localization of the AvDGK proteins. The secondary structures of the AvDGK proteins were predicted using SOPMA (http://npsa-pbil.ibcp.fr/cgi-bin/npsa_automat.pl?page=npsa_sopma.html) (accessed on 29 November 2023) [43]. Furthermore, we utilized the online tool Phyre2 [44] (<http://www.sbg.bio.ic.ac.uk/phyre2/html/page.cgi?id=index>) (accessed on 1 February 2024) for protein homology modeling and the generation of 3D models of AvDGK proteins using default parameters. The protein domains were analyzed using the SMART database, and the domain structures in all AvDGK proteins were plotted using IBS 1.0.3 software [45].

2.3. Phylogenetic Analyses and Multiple Sequence Alignment of AvDGK Proteins

The 7 AtDGK protein sequences were downloaded from the TAIR database (<https://www.arabidopsis.org/>) (accessed on 31 October 2023), 7 ZmDGKs were obtained from the maize protein database (*Z. mays*, <http://www.maizegdb.org/>) (accessed on 9 November 2023), 7 PtDGKs were obtained from Phytozome v13 (*P. trichocarpa*, <https://phytozome-next.jgi.doe.gov/>) (accessed on 9 November 2023) [46], and 9 AchDGKs were obtained by BLASTp from the whole protein sequences of *Actinidia chinensis* cv. 'Hongyang' with AtDGKs. Multiple sequence alignment of these DGK proteins was performed using the Clustal W method in DNAMAN 8.0 software (Lynnon Biosoft, Vaudreuil, QC, Canada) with default parameters. Based on the result of sequence alignment, the phylogenetic tree was constructed using MEGA 7.0 software (Mega Limited, Auckland, New Zealand) with the neighbor-joining (NJ) method. A bootstrap analysis with 1000 replicates was performed, and the online web tool iTOL (<https://itol.embl.de/>) (accessed on 10 November 2023) was utilized for tree visualization [47].

2.4. Analysis of Gene Structures and Conserved Motifs

The coding sequences (CDS) and their corresponding genomic sequences of AvDGK genes were retrieved from *A. valvata* genomic files. The conserved motifs of AvDGK protein sequences were predicted using the MEME (MEME 5.5.4) online tool (<https://meme-suite.org/meme/tools/meme>) (accessed on 1 November 2023) [48] and the numbers of motifs were set to 10. The gene structures and conserved motifs of AvDGK were visualized using TBtools II software [49].

2.5. Chromosome Location, Gene Duplication, and a Collinearity Analysis of AvDGK Genes

The chromosomal localization of the AvDGK genes was achieved from a gff3 file of the genome and mapped on the chromosomes using MG2C v2.1 online software (http://mg2c.iask.in/mg2c_v2.1/) (accessed on 7 November 2023) [50]. Gene duplication events were identified by generating syntenic blocks within and between kiwifruit genomes using the MCScanX program with default parameters [51]. The collinearity of the DGK family members within *A. valvata* genomes and between *A. valvata* and *A. thaliana*, as well as between *A. valvata* and *A. chinensis*, was determined using TBtools software [49]. The Ka

(synonymous) and Ks (nonsynonymous) substitution rates in the duplicated *DGK* gene pairs were calculated using TBtools software [49]. A ratio of Ka/Ks of less than 1 suggests the presence of purifying selection, whereas a ratio greater than 1 implies positive selection and a ratio of exactly 1 is characteristic of neutral selection [52].

2.6. Cis-Regulatory Element Prediction and an Analysis of Promoters

The 2000 bp upstream sequences of *AvDGK* genes were extracted from the genomic DNA sequences and selected as the promoter region. The promoter sequences were submitted to PlantCARE (<https://bioinformatics.psb.ugent.be/webtools/plantcare/html/>) (accessed on 1 November 2023) to predict the *cis*-regulatory elements [53]. TBtools was used in visualizing the results of the analysis.

2.7. Gene Expression Analysis of *AvDGKs*

Raw RNA-seq data of the *AvDGK* genes in the flesh at different developmental stages of the fruit and in roots under salt stress were downloaded from NCBI (<https://www.ncbi.nlm.nih.gov/>) (accessed on 1 November 2023) with the following accession number (PRJNA984935, PRJNA726156). The quantification of gene expression was depicted using the log₂-transformed FPKM values, which were calculated using Kallisto and visualized using TBtools [49,54].

2.8. Plant Materials and Treatments

Two-year *A. valvata* seedlings were provided by the Guangxi Key Laboratory of Plant Functional Phytochemicals and Sustainable Utilization and grown under normal conditions for three months. For the waterlogging experiment, each three potted seedlings were placed in a plastic container (61 × 48 × 36 cm) filled with tap water. The seedlings were submerged to a final depth range of 3~5 cm beneath the water surface for 5 days under normal light/dark conditions. Fresh root samples were collected at 0, 6, 24, and 120 h after the waterlogging treatment and immediately frozen in liquid nitrogen for further analyses. For each sample, a set of three replicates was established, with each replicate comprising three individual seedlings.

2.9. RNA Extraction and qRT-PCR Analysis

The total RNA of the root samples was extracted using the RNAprep Pure Plant Kit (TIANGEN, Beijing, China). The FastKing RT Kit With gDNase (TIANGEN) was employed to reverse the RNA into cDNA. Following the protocol for SuperReal PreMix Plus (SYBR Green) (TIANGEN), each 20 µL reaction mixture contained 1 µL of template cDNA, 10 µL of the 2 × SuperReal PreMix Plus (SYBR Green), 0.6 µL of each primer, and 7.8 µL of ddH₂O. The reaction conditions comprised a pre-denaturation stage at 95 °C for 5 min, followed by 40 cycles of denaturation at 95 °C for 10 s, annealing at 60 °C for 20 s, and extension at 72 °C for 20 s. The *A. valvata* actin gene (*AVa07g00333*) was used as the reference gene. The relative expression levels were calculated using the 2^{-ΔΔCT} method [55] and three duplicates were performed. All primer pairs used for the RT-PCR are listed in Table S1.

2.10. Statistical Analysis

All statistical analyses were performed with Microsoft Excel 2021. The significance levels of the data were ascertained through a one-way ANOVA in SPSS (ANCOVA; SPSS26, SPSS Inc., Chicago, IL, USA), and * *p* < 0.05 and ** *p* < 0.01 indicated that the differences were significant and extremely significant. The data are presented as the mean ± standard deviation (±SD). Each treatment was repeated three times.

3. Results

3.1. Genome-Wide Identification of *DGK* Genes in *A. valvata*

We identified a total of 18 putative *AvDGK* family members from the genome of *A. valvata*, and their domains were confirmed using the NCBI CDD and SMART databases.

Finally, all 18 candidate *AvDGK* genes were proven to contain both functional domains and identified from the kiwifruit genome. Based on their chromosome positions, they were named as *AvDGK5a/b*, *AvDGK7a/b*, *AvDGK12a/b*, *AvDGK13a/b*, *AvDGK16a/b*, *AvDGK17a/b*, *AvDGK18a/b*, *AvDGK19a/b*, and *AvDGK23a/b* (Figure 1 and Table S2). The CDS lengths of the *AvDGK* genes ranged from 1371bp to 2205bp and the lengths of the proteins were 456–734 amino acids (Table 1). Their molecular weights ranged from 50.84 to 81.06 kDa, and the pI values ranged from 6.31 to 9.16. The predicted subcellular localization of the proteins was in the nucleus, chloroplast, and cytoplasm (Table 1).

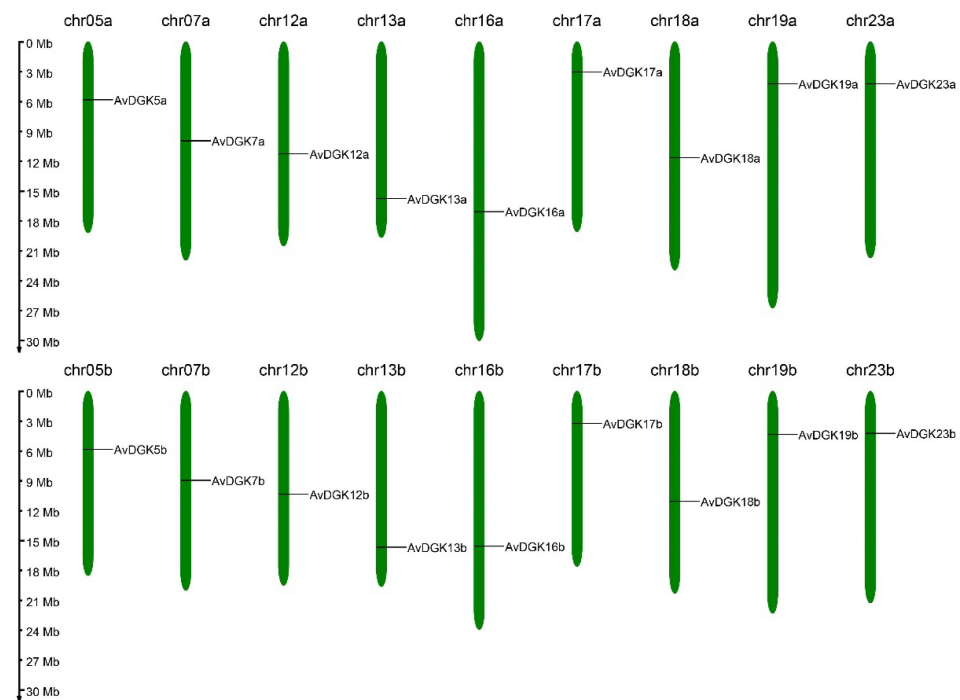


Figure 1. Chromosomal localization of *AvDGK* genes.

Table 1. The characteristics of the *DGK* family members in *A. valvata*.

Gene Name	Gene ID	CDS Length (bp)	Number of Amino Acids (aa)	Molecular Weight (kDa)	pI	Subcellular Localization
<i>AvDGK5a</i>	Ava05g00367	2139	712	79.50	8.62	Nucleus
<i>AvDGK5b</i>	Avb05g00366	2139	712	79.31	8.74	Nucleus
<i>AvDGK7a</i>	Ava07g00406	2139	712	79.24	8.14	Nucleus
<i>AvDGK7b</i>	Avb07g00371	2139	712	79.39	8.14	Nucleus
<i>AvDGK12a</i>	Ava12g00623	1449	482	54.05	8.57	Chloroplast. Cytoplasm. Nucleus
<i>AvDGK12b</i>	Avb12g00588	1392	463	51.84	7.06	Cytoplasm
<i>AvDGK13a</i>	Ava13g01333	1419	472	53.55	9.16	Chloroplast
<i>AvDGK13b</i>	Avb13g01246	1419	472	53.28	8.68	Chloroplast. Cytoplasm. Nucleus
<i>AvDGK16a</i>	Ava16g01104	1446	481	53.40	6.84	Chloroplast
<i>AvDGK16b</i>	Avb16g01069	1437	478	53.14	6.87	Chloroplast
<i>AvDGK17a</i>	Ava17g00287	1473	490	54.90	6.39	Chloroplast. Cytoplasm
<i>AvDGK17b</i>	Avb17g00295	1473	490	54.95	6.31	Cytoplasm. Nucleus
<i>AvDGK18a</i>	Ava18g00909	1446	481	53.53	6.72	Chloroplast
<i>AvDGK18b</i>	Avb18g00884	1371	456	50.84	6.41	Chloroplast
<i>AvDGK19a</i>	Ava19g00482	2199	732	80.77	6.32	Nucleus
<i>AvDGK19b</i>	Avb19g00480	2205	734	81.06	6.50	Nucleus
<i>AvDGK23a</i>	Ava23g00486	2205	734	80.91	6.44	Nucleus
<i>AvDGK23b</i>	Avb23g00493	2205	734	80.83	6.41	Nucleus

3.2. Phylogenetic Analysis and Multiple Sequence Alignment of DGK Genes

To elucidate the phylogenetic relationships and functional differences of the 18 *Av*DGKs, the phylogenetic tree of these DGK proteins was constructed. The results showed that the 18 *Av*DGK proteins were divided into three clusters (Figure 2). Cluster I included *Av*DGK5a/b, *Av*DGK7a/b, *Av*DGK19a/b, and *Av*DGK23a/b; cluster II contained *Av*DGK16a/b and *Av*DGK18a/b; cluster III consisted of *Av*DGK12a/b, *Av*DGK13a/b, and *Av*DGK17a/b. The grouped results of the phylogenetic tree were confirmed by the amino acid similarities between *At*DGKs and *Av*DGKs (Figure S1). The phylogenetic tree also revealed that the *Av*DGKs had high homology with the DGKs in *A. chinensis* ‘Hongyang’, and the *Av*DGKs are more closely related to the *Ach*DGKs located in the same chromosome of kiwifruit than to the DGKs of other plants.

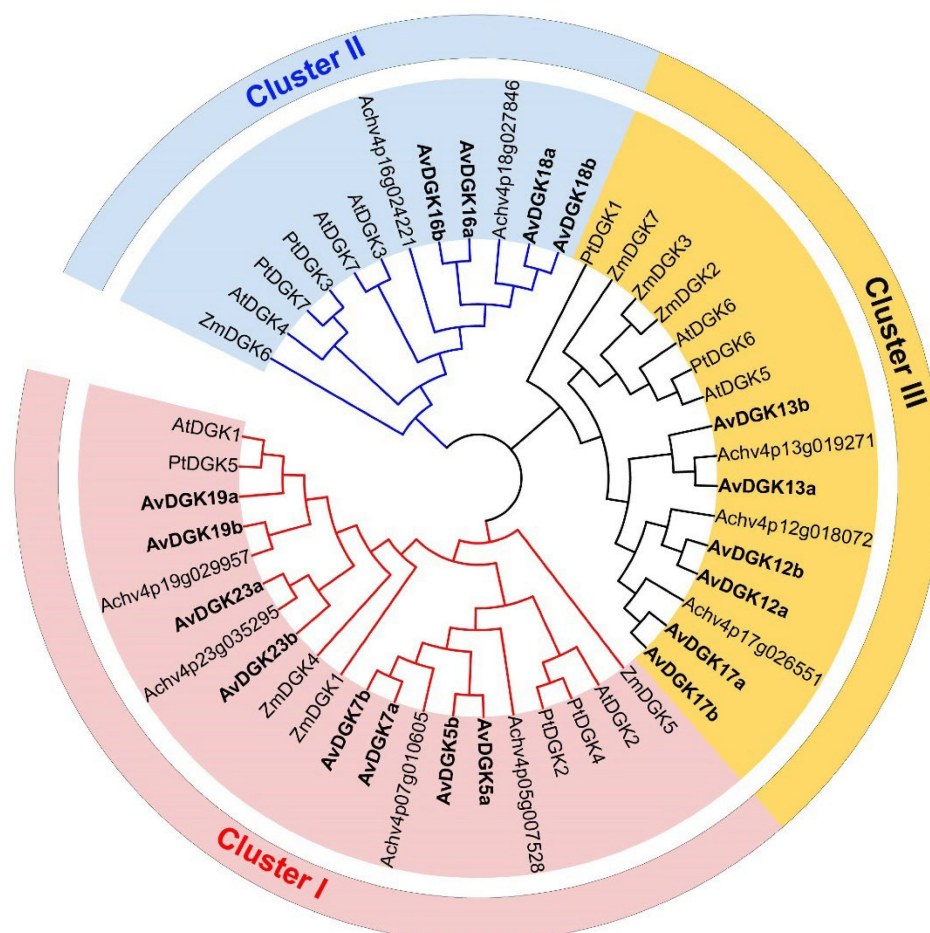


Figure 2. A phylogenetic tree analysis of the DGK proteins from *A. valvata* (*Av*), *A. chinensis* (*Ach*), *A. thaliana* (*At*), *P. trichocarpa* (*Pt*), and *Z. mays* (*Zm*). The protein sequences were aligned with the Clustal W program using MEGA 7.0 and the phylogenetic tree was constructed using the neighbor-joining method with 1000 bootstrap replicates. The *Av*DGK genes are highlighted in bold type.

To identify the conserved sequences in the *Av*DGKs, multiple sequence alignment was performed. According to the alignment, a diacylglycerol kinase catalytic (DAGKc) domain (Figure 3A), a diacylglycerol kinase accessory (DAGKa) domain (Figure 3B), and two DAG/PE-binding domains (Figure 3C) were shown. The alignment revealed that almost all DGKs, except for the *At*DGK2, *Av*DGK5a/b, *Av*DGK7a/b, and *Av*DGK13a/b, contained the predicted ATP-binding site, with a GXGXXG consensus sequence (where G represents glycine and X represents any other amino acid) in the DAGKc domain. Furthermore, glycine (G) was replaced by alanine (A) in *At*DGK2, *Av*DGK5a/b, and *Av*DGK7a/b and by lysine (K) in *Av*DGK13a/b. The two C1 domains observed in cluster I DGKs harbored the

sequences HX14CX2CX19~22CX2CX4HX2CX7 and HX18CX2CX16CX2CX4HX2CX11C, respectively (Figure 3D). Additionally, the upstream basic regions and the extended cysteine-rich (extCRD)-like domain were extremely conserved in cluster I.

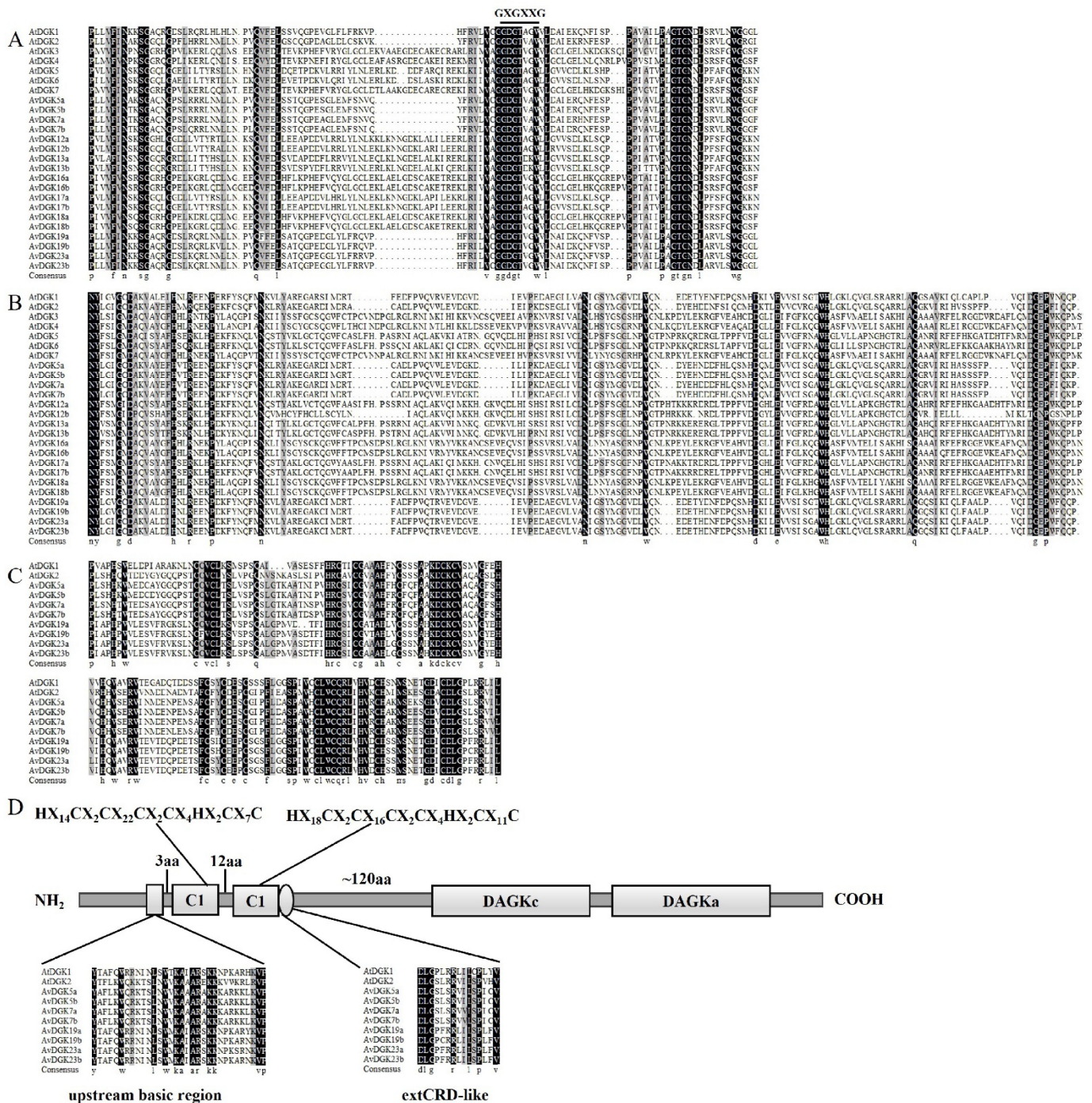


Figure 3. Multi-sequence alignment and a domain analysis of AtDGK and AvDGK proteins: (A) DAGKc domain, where the predicted ATP-binding site with a GXXGXXG consensus sequence is shown below the DAGKc domain; (B) DAGKa domain; (C) DAG/PE-binding domains in DGKs; (D) a schematic diagram of AvDGK genes in cluster I. The conserved C6/H2 cores, the upstream basic regions, and the extended cysteine-rich (extCRD)-like domain are shown in the schematic diagram.

3.3. Functional Domain, Secondary Structure, and 3D Modeling of AvDGKs

To further explore the protein domains in all AvDGKs, the functional domains of the AvDGKs were predicted (Figure 4). The results showed that all DGKs had both a DAGKc

domain and a DAGKa domain. Additionally, the DGK proteins in cluster I (AvDGK5a/b, AvDGK7a/b, AvDGK19a/b and AvDGK23a/b) also contained two C1 domains. Based on the starting and ending positions of the domains, AvDGK19a/b exhibited greater similarities with AvDGK23a/b than other DGKs in cluster I. The domain position and distribution of AvDGK5a/b were completely consistent with AvDGK7a/b. Similar domain positions and distributions were found in the DGKs in the same cluster.

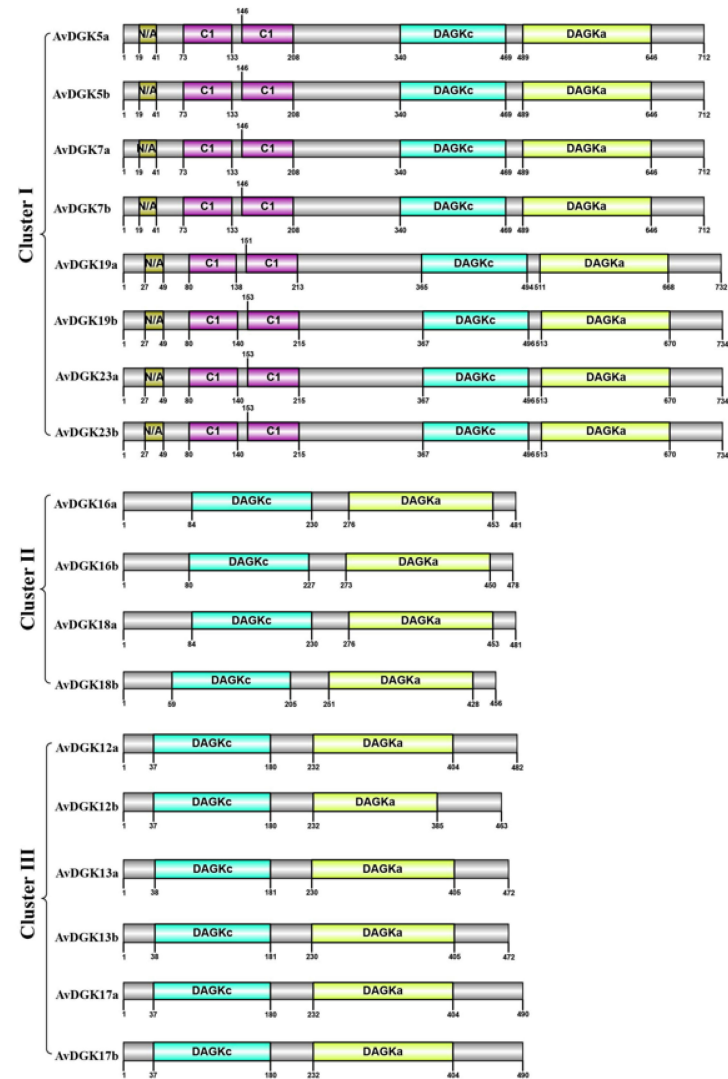


Figure 4. Distribution of the function domains in AvDGK proteins. The numbers up and down the protein indicate the position of each domain in the protein. N/A represented an unidentified transmembrane domain distributed in AvDGK proteins.

To develop a better understanding of the DGK protein structure, the secondary structure of the AvDGKs were predicted. The secondary structure of the AvDGK proteins was predominantly composed of alpha helices, extended strands, beta turns, and random coils (Figure S2 and Table S3). The analysis showed that the random coils accounted for the largest percentage of secondary structures among all AvDGK proteins, followed by the alpha helix and extended strands, while the beta turns accounted for less than 6.0%. Additionally, the 3D models of all AvDGKs proteins were predicted (Figure 5). Similar 3D structures were found in AvDGKs, and the composition and position of the secondary structure could be clearly observed.

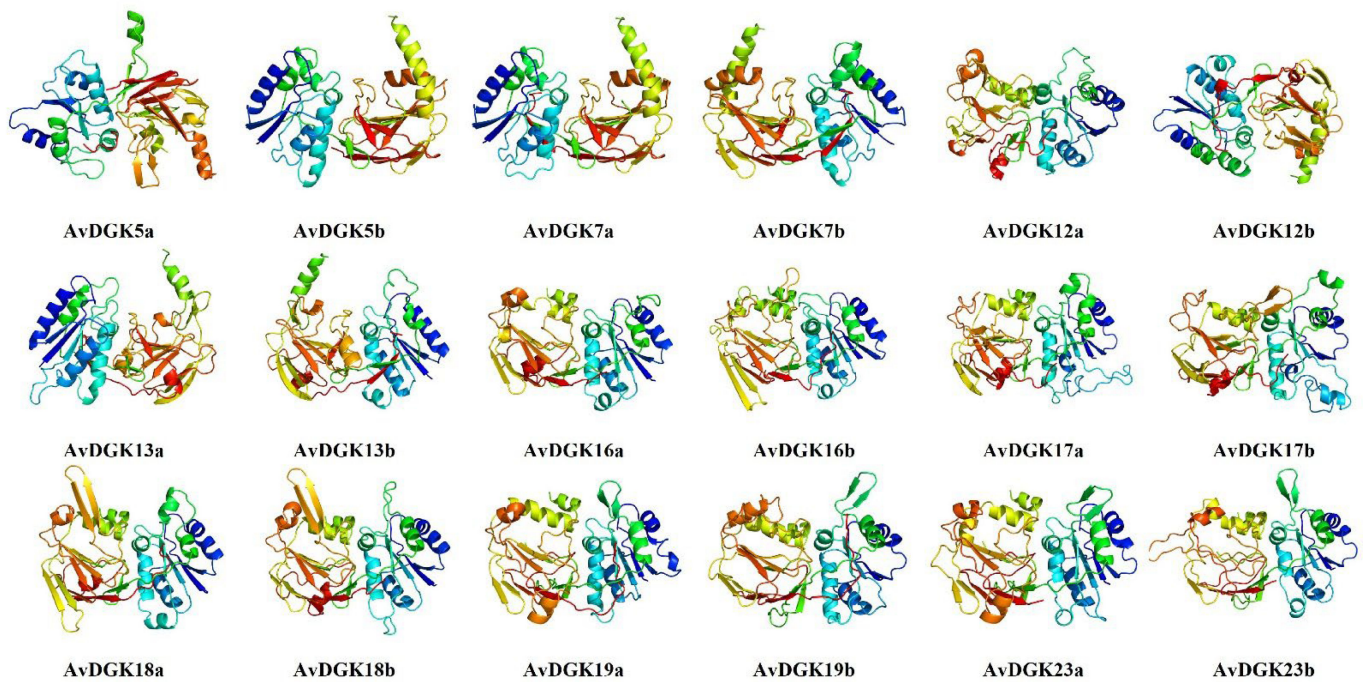


Figure 5. The 3D models of AvDGK proteins. The 3D models were constructed using the online Phyre2 server with default mode.

3.4. Gene Structure, Domain, and Conserved Motif Analysis of AvDGKs

To investigate the diversity and differentiation of the AvDGKs, we further analyzed the gene structure, conserved domains, and motifs of the AvDGK family. A total of 10 different conserved motifs, labeled as motif 1 to motif 10, were identified in the AvDGKs (Figure 6B and Figure S3). A similar motif distribution was observed within each cluster. According to the results, the AvDGKs from cluster I contained a maximum of 10 motifs, while the AvDGKs from cluster II contained a minimum 6 motifs (Figure 6B). The members of cluster III contained one additional motif compared to the members of cluster II, namely motif 10. The protein domains of the AvDGKs are clearly shown in Figure 6C. All AvDGKs had a DAGKc domain and a DAGKa domain, and two C1 domains were conserved in cluster I DGKs (Figure 6C). The gene structure of the AvDGKs could provide insights for their classification and functional diversification. The AvDGKs genes belonging to cluster I possessed a smaller number of exons compared to other AvDGKs genes, which all contained 7 exons and 6 introns (Figure 6D and Figure S4). The cluster II members (*AvDGK16a/b* and *AvDGK18a/b*) all contained 12 exons and 11 introns, whereas the exon numbers from cluster III varied from 11 to 13 (Figure 6D and Figure S4).

3.5. Synteny and Gene Duplication Analysis of AvDGKs

To determine the expansion patterns of the DGK gene family, we undertook a collinearity assessment aimed at detecting gene duplication events for DGK genes in *A. valvata*. A total of 29 duplicated gene pairs were identified in the *A. valvata* genome (Figure 7 and Table S4). As a tetraploid, the *A. valvata* genome comprised two subgenomes (a and b). Among them, there were 5 duplicated gene pairs each within subgenome a and subgenome b of *A. valvata*, and 19 duplicated gene pairs between subgenome a and subgenome b. Then, we estimated the selection pressure of the replication gene pairs. The results showed that the Ka/Ks ratios for all duplicated gene pairs varied between 0.11 and 0.85, indicating that the duplicated gene pairs in the kiwifruit underwent purifying selection (Table S4). Additionally, the data show that the gene duplication events within *A. valvata* occurred between 4.67 to 76.36 million years ago (MYA) (Table S4).

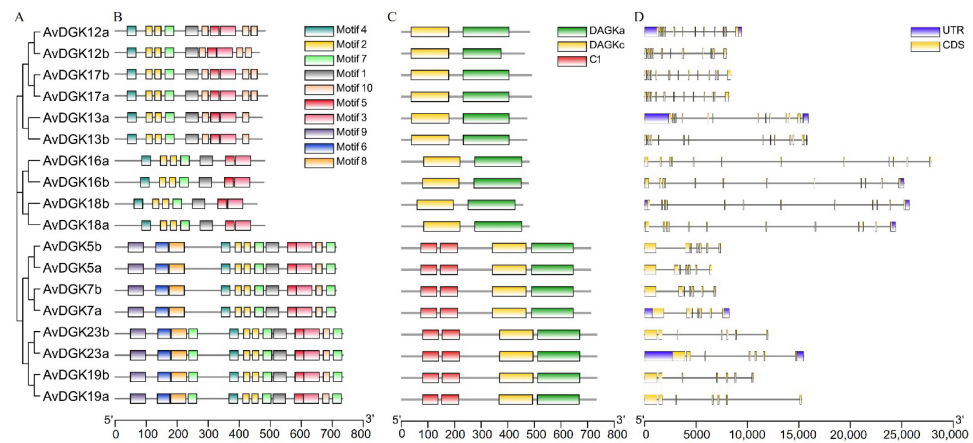


Figure 6. The phylogenetic tree, motif composition, domain location, and gene structure of the *AvDGKs*. (A) The phylogenetic tree of the *AvDGK* proteins. (B) The conserved motif distribution of the *AvDGK* proteins. (C) The domain location of the *AvDGK* proteins. (D) The gene structure of the *AvDGK* genes, where yellow indicates the exons, gray lines indicate the introns, and purple shows the untranslated 5' and 3'-regions.

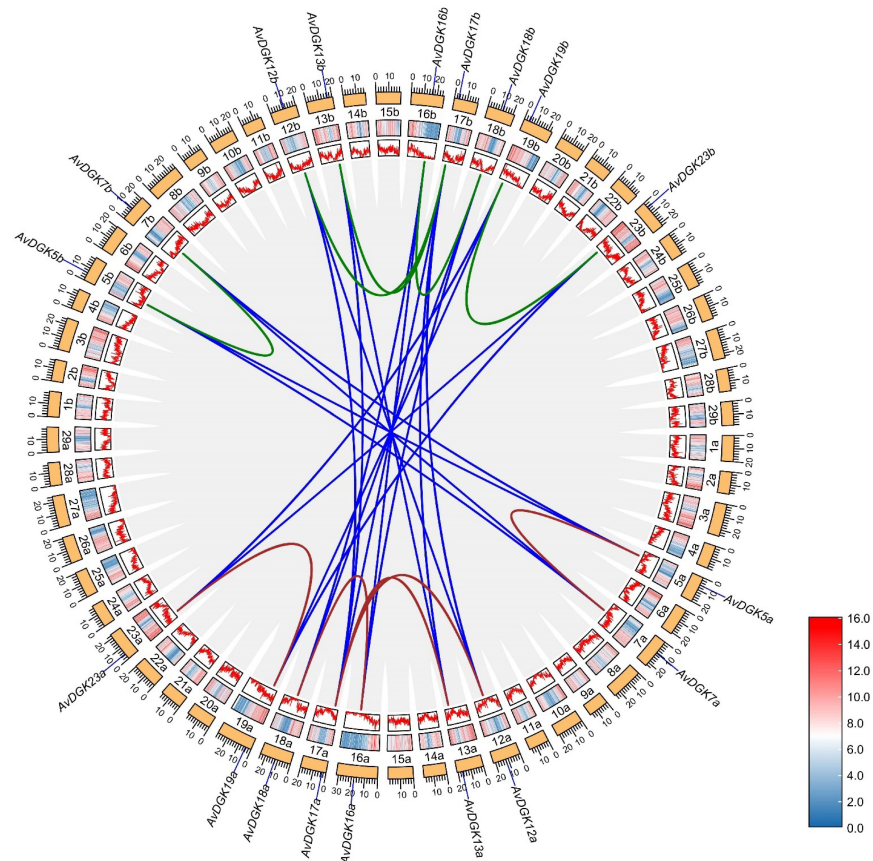


Figure 7. A collinearity analysis of *AvDGKs*. Grey lines indicate all duplicate genes, while other different colored lines indicate the duplicated *DGK* gene pairs within and between *A. valvata* subgenomes. The heatmap and line graph indicate gene density.

To further understand the evolutionary origins and orthologous relationship of the *DGK* gene family, a collinearity analysis was performed among *A. valvata*, *A. thaliana*, and *A. chinensis* ‘Hongyang’ (Figure 8). Nineteen gene pairs were found between between *A. valvata* subgenome a and subgenome b (Figure 8A). Eighteen gene pairs were found between *A. valvata* subgenome and *A. chinensis* ‘Hongyang’ (Figure 8B). The difference

was that 11 and 10 gene pairs were found between *A. thaliana* with *A. valvata* subgenome a and subgenome b, respectively (Figure 8C). The collinearity analysis offers a deeper understanding of the evolutionary dynamics and functional divergence of the *DGK* gene family in *A. valvata* and the related species.

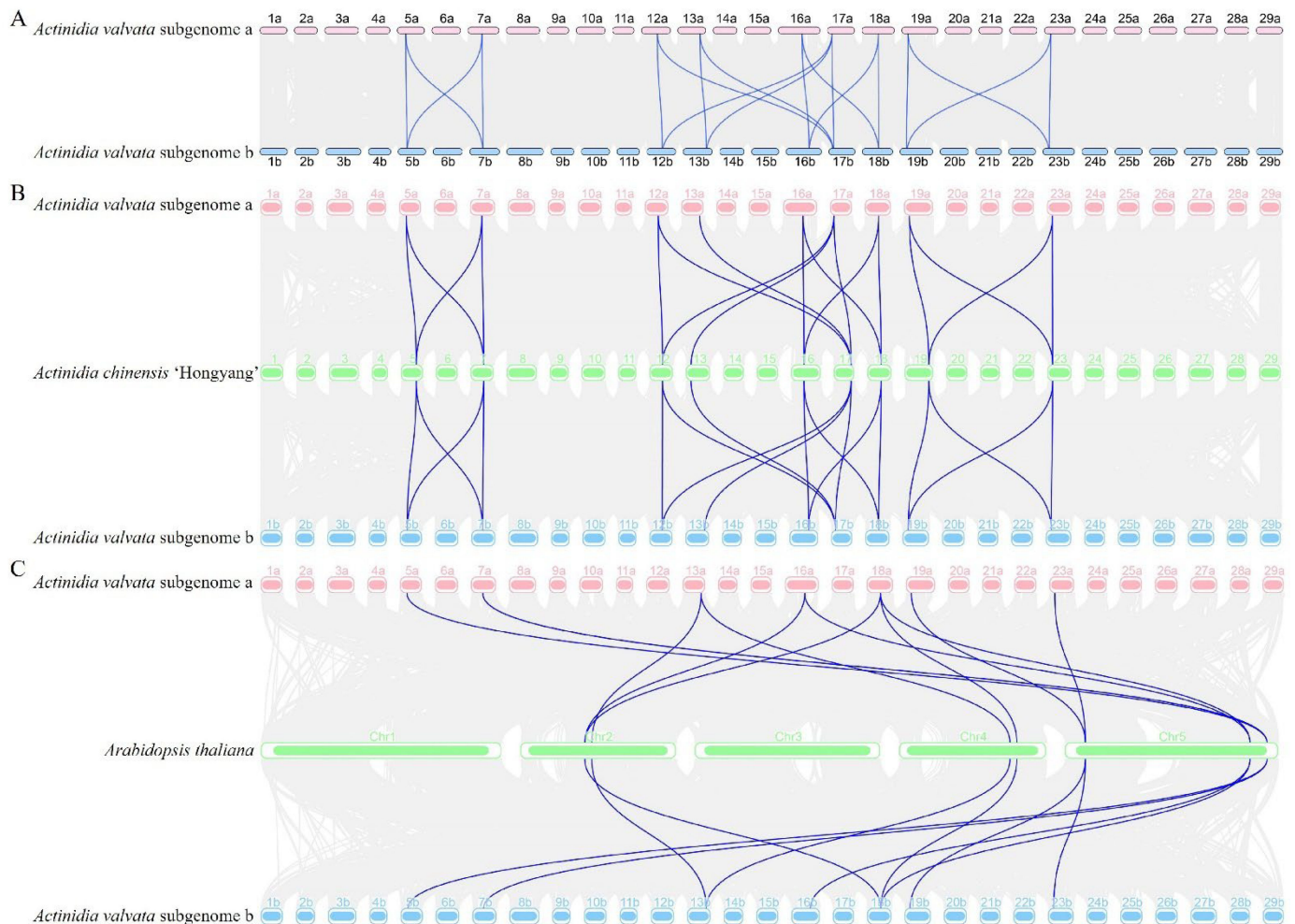


Figure 8. A multiple collinearity analysis between *A. valvata*, *A. thaliana*, and *A. chinensis* 'Hongyang'. (A) The collinearity analysis between *A. valvata* subgenome a and b. (B) The collinearity analysis between *A. valvata* subgenome and *A. chinensis* 'Hongyang'. (C) The collinearity analysis between *A. valvata* subgenome and *A. thaliana*. The grey lines in the background represent all syntenic blocks between *A. valvata* subgenomes and other plants, while the blue lines highlight the *DGK* genes orthologous in *A. valvata* subgenomes and other plants. The different colored columns represent the chromosomes.

3.6. Analysis of Cis-Elements in the Promoters of *AvDGK* Genes

To explore the possible regulatory patterns of the *AvDGK* genes, the putative cis-elements in the promoter regions of all *AvDGK* genes were analyzed (Figure 9). The distribution and numbers of these cis-elements exhibited that the light responsiveness element was the most commonly occurring (Figure 9A). The phytohormone-responsive cis-acting elements were also widely distributed, especially the methyl jasmonate (MeJA) responsiveness element, which was present in almost all *AvDGK* genes. However, only six *AvDGK* promoters contained salicylic acid (SA) responsiveness elements. Moreover, the cis-acting elements related to stress responses, such as wound stress responsiveness, drought responsiveness, low-temperature responsiveness, anaerobic induction, defense, and stress responsiveness, were also found in promoters of *AvDGK* genes (Figure 9A). Notably, hypoxia induces the expression of almost all *AvDGK* genes, except for *AvDGK18b*

and *AvDGK19a*. Furthermore, 66.67% of the *AvDGK* genes exhibited responsiveness to drought stress, while *AvDGKs* within cluster II were implicated in the response to low-temperature stress.

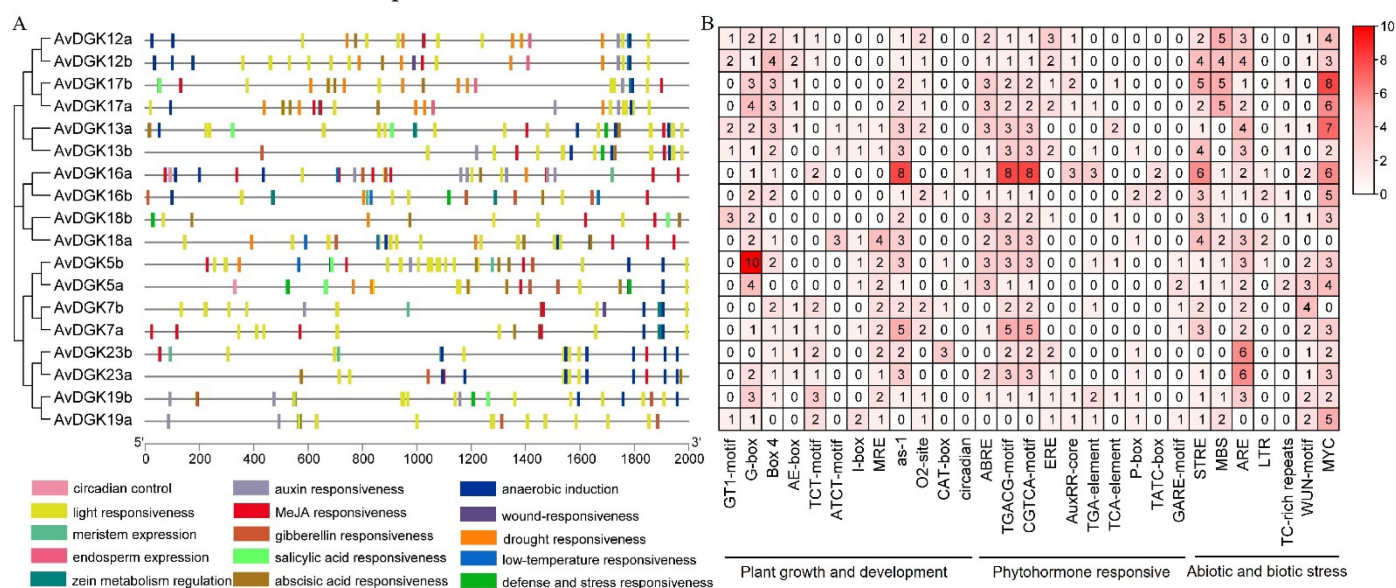


Figure 9. The *cis*-element analysis of the *AvDGKs*: (A) distribution of *cis*-regulatory elements in the promoter regions, with each colored rectangle depicting a distinct type of *cis*-element; (B) statistics on the number of *cis*-acting elements associated with plant growth and development and phytohormone and stress responses in the promoter region of *AvDGK* genes.

We also identified the number and types of *cis*-elements, which were classified into 3 classes (Figure 9B). According to their functions, they were divided into plant growth and development, phytohormone-responsive, and abiotic and biotic stress groups. In the plant growth and development category, there were 41 G-boxes (light responsiveness), of which *AvDGK5b* accounted for 10 (Figure 9B). In the phytohormone responsive categories, the CGTCA motif (MeJA responsiveness) and TGACG motif (MeJA responsiveness) were two most widely distributed, being present in almost all of the 18 genes except *AvDGK19a* (Figure 9B). Additionally, in the abiotic and biotic stress categories, the number of MYC (multi-stress responsiveness) was the most distributed except *AvDGK5a* and *AvDGK18a* (Figure 9B).

3.7. Expression Patterns of *AvDGKs* in Kiwifruit

To investigate the expression patterns of the *AvDGKs* in kiwifruit, we analyzed the expression levels of the *AvDGK* genes in the flesh of the fruit at different developmental stages and in the roots under salt stress by utilizing two transcriptome datasets. The expression of the *AvDGKs* could be estimated across four fruit stages—stage 1 (mature green fruit stage), stage 2 (breaker fruit stage), stage 3 (color change fruit stage), and stage 4 (ripe fruit stage) (Figure 10A). The expression profile revealed that *AvDGK16a/b*, *AvDGK17b*, and *AvDGK18b* exhibited higher expression levels across different fruit developmental stages. In contrast, genes like *AvDGK7a/b* and *AvDGK13a/b* showed lower expression levels. Additionally, the *AvDGKs* presented different expression profiles during the fruit development stage (Figure 10A). *AvDGK12a/b* and *AvDGK18a/b* showed decreased expression during fruit development, while an increase in expression at the breaker fruit stage was observed in most other *AvDGK* genes (Figure 10A). The expression levels of the *AvDGKs* in the roots were evaluated after salt treatment for 0 h, 12 h, 24 h, and 72 h using the transcriptome data (Figure 10B). The heatmap results showed that the expression of *AvDGK5a/b*, *AvDGK16a/b*, *AvDGK17a/b*, *AvDGK18a/b*, and *AvDGK19a/b* was downregulated in response to the salt treatment, indicating that the expression of *DGK* in the roots was inhibited under salt stress (Figure 10B).

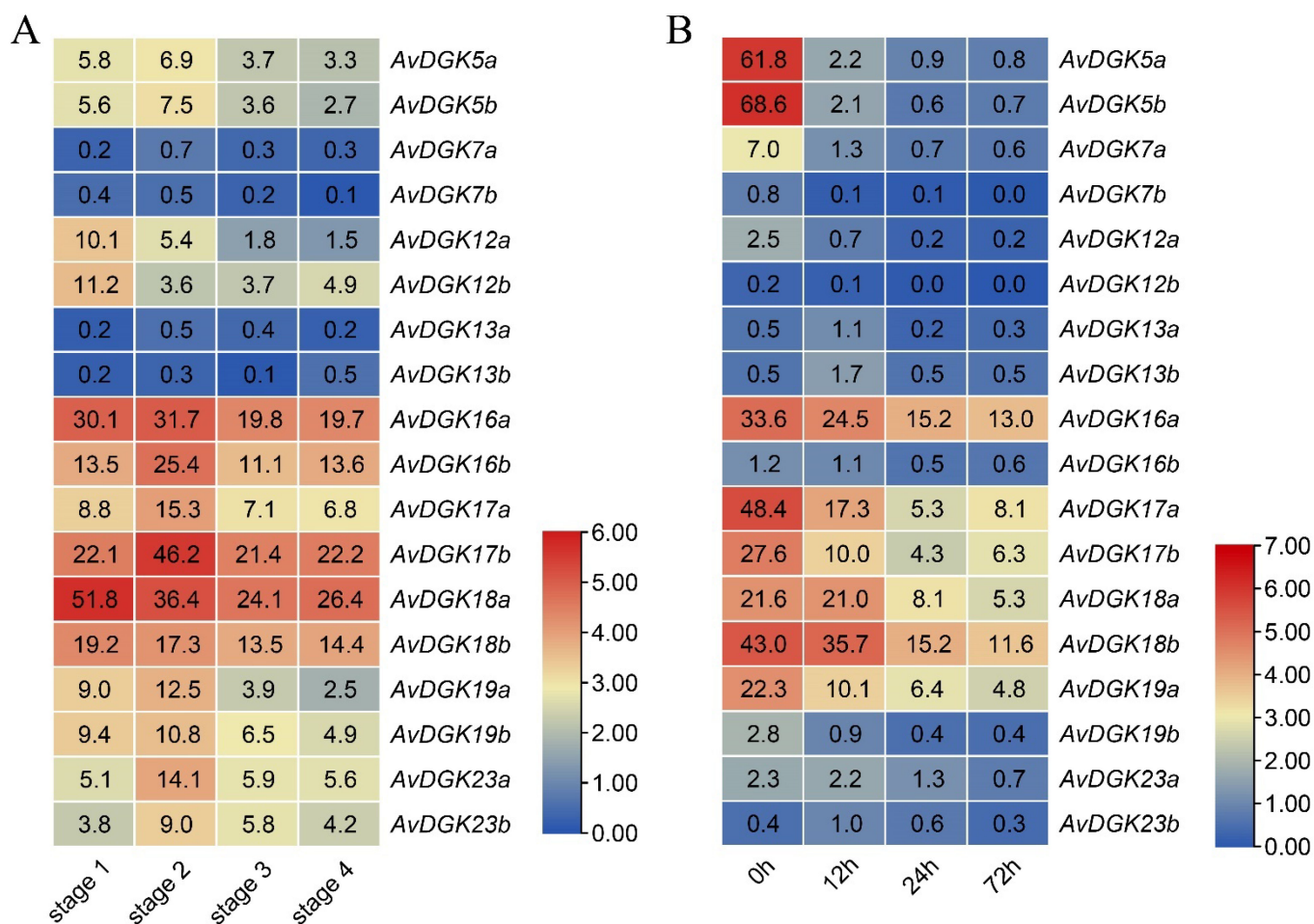


Figure 10. Expression profiles of *AvDGKs* in different fruit stages and under salt stress: (A) expression profiles of *AvDGKs* in fruit flesh at stage 1 (mature green fruit stage), stage 2 (breaker fruit stage), stage 3 (color change fruit stage), and stage 4 (ripe fruit stage); (B) expression profiles of *AvDGKs* in the roots under salt stress at 0 h, 12 h, 24 h, and 72 h.

3.8. RT-qPCR of *AvDGKs* under Waterlogging Stress at Different Times

To further evaluate the role of the *AvDGKs* in the response to waterlogging stress, we performed an RT-qPCR to obtain insights into the expression patterns of the *AvDGKs* in the roots under waterlogging stress. As shown in Figure 11, the relative expression levels of 15 *AvDGKs* were significantly changed after the treatment. Of these, the waterlogging stress significantly induced the expression of *AvDGK12a*, *AvDGK12b*, and *AvDGK18b* (Figure 11). Interestingly, the expression levels of *AvDGK12a* and *AvDGK12b* were slightly different at different treatment times. *AvDGK12b* was rapidly induced by the submergence treatment at 6 h and displayed a trend of decline following the waterlogging stress. In contrast, significant upregulation of the gene expression for *AvDGK12a* was observed until the submergence treatment at 120 h. The expression pattern of *AvDGK18b* post-submergence treatment was similar to that of *AvDGK12b*. Conversely, no significant change in gene expression was detected for *AvDGK18a* following the submergence treatment. The result suggested that *AvDGK12b* and *AvDGK18b* played a key role in the short-term response, while *AvDGK12a* may be involved in regulating the long-term waterlogging stress response. During the stress, *AvDGK5b*, *AvDGK7a*, and *AvDGK13b* and *AvDGK16a*, *AvDGK19a/b*, and *AvDGK23a/b* showed similar expression patterns, whereby they sharply decreased to a relatively lower expression level at 6 h and 24 h, respectively, and were upregulated slightly at 120 h (Figure 11). Similarly, the relative expression levels of *AvDGK5a*, *AvDGK7b*, *AvDGK13a*, and *AvDGK16b* were significantly reduced and remained at a relatively low

level during the submergence stress. The waterlogging stress had no effect on the expression of *AvDGK17a/b*.

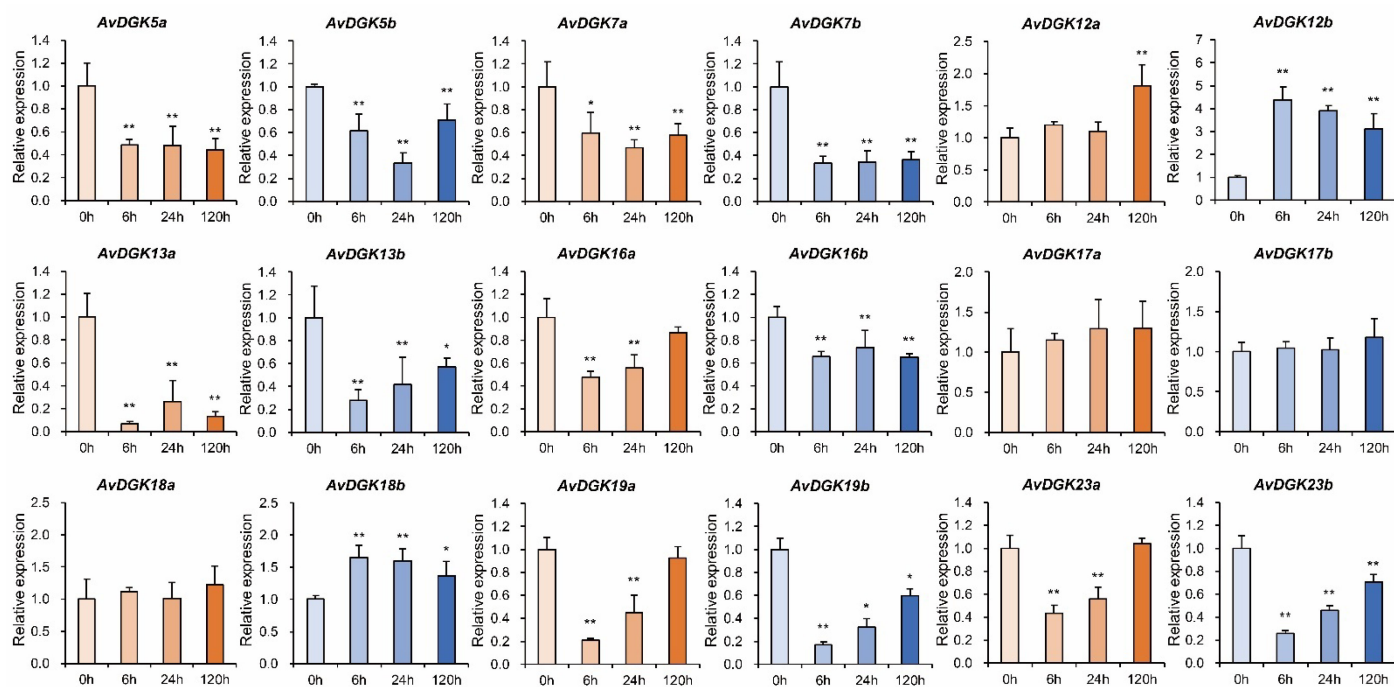


Figure 11. The relative expression levels of *AvDGKs* in the roots under waterlogging stress at different times. Data are shown as means \pm SD ($n = 3$) and statistical significance is indicated by * ($p < 0.05$) and ** ($p < 0.01$).

4. Discussion

The ability to sense and respond to various environmental stimuli is essential for the growth, development, and survival of plants. Diacylglycerol kinase (DGK) plays a pivotal role in this process by regulating the levels of two crucial signaling molecules, diacylglycerol (DAG) and phosphatidic acid (PA) [12,28]. After the lipid phosphorylation of DAG, PA is rapidly produced and accumulates in response to a variety of stresses, such as cold stress, salt stress, hypoxia stress, and submergence [29,56,57]. Upon submergence, it was reported that the DGKs and PA derived from DGKs were critical for regulating plant acclimation to submergence [29]. As a submergence-tolerant germplasm, an increasing number of recent studies on *A. valvata* have focused on understanding the plant's mechanism of regulating its tolerance to submergence [35–37,58–60]. However, no reports have involved the identification and functional analysis of *DGK* gene family members in the waterlogging tolerance of *A. valvata*. In this study, we identified 18 *AvDGK* members within the *A. valvata* genome, which were located on 18 different chromosomes. The number of *AvDGK* genes identified in the *A. valvata* genome was higher than the numbers found in *A. thaliana* (7 *AtDGKs*) [14], *Z. mays* (7 *ZmDGKs*) [21], *M. domestica* (8 *MdDGKs*) [19], and *P. trichocarpa* (7 *PtDGKs*) [22] but less than those in *T. aestivum* (24 *TaDGKs*) [18] and *B. napus* (21 *BnaDGKs*) [17], which may be due to the differences in the sizes of the genomes. The *AvDGKs* encoded proteins ranging from 456 to 734 amino acids, and these proteins were subcellularly located in the nucleus, chloroplast, and cytoplasm. The physicochemical properties and subcellular localization of the *AvDGKs* were similar to in the previous *DGKs* identified from other plants [16–20,22]. The grouping and evolutionary relationships of the *DGK* gene family were determined via multiple sequence alignment and phylogenetic tree construction among monocots and dicots. The *AvDGKs* were classified into three clusters, I, II, and III, and this classification was confirmed via domain prediction and an analysis. The classification of the *AvDGKs* was consistent with previously published reports performed in other plants and supported the domain conservation and sequence similarity of

DGKs in plants. In plants, the DGKs in cluster I show a relatively complex domain distribution. They possess the conserved catalytic kinase domain and two C1-type domains, which are cysteine-rich domains thought to be responsible for binding the substrate DAG [14]. In addition, an upstream basic region and an extended cysteine-rich (extCRD)-like domain was also found next to the C1 domain. In contrast, cluster II and cluster III DGKs lack the two C1 domains but still retain the conserved kinase domain. The domain analysis showed that all three clusters displayed structural characteristics consistent with previous findings, indicating that high conservation of functional domains across different species persists in the evolution of DGKs.

Besides the conserved domains, similar exon–intron numbers, motif compositions, and subcellular locations were found within the clusters. The gene structures of *AvDGK* members in clusters I and II revealed that they contained seven and twelve exons, respectively; the same numbers of exon were also found in wheat [18], common bean [16], soybean [20], and poplar [22]. The conserved exon–intron structure in clusters I and II indicates that the DGKs possibly come from a common ancestor, and DGK genes have experienced a significant influence from recurrent gene duplication events throughout evolutionary history [61]. Additionally, different intron and exon patterns were found in *AvDGK* belonging to cluster III, suggesting that the ancestral *AvDGK* gene is likely to have undergone several rounds of intron loss and gain during evolution [62]. These structural differences in cluster III might confer distinct functional properties.

Diverse gene functions are affected significantly by the *cis*-element located in the promoter regions. Previous studies have reported that *cis*-elements on the promoters of DGKs are associated with multiple stresses such as drought, cold stress, and wound stress and hormone responses such as ABA, SA, and MeJA [16–18,21,22]. Some of the predictions were confirmed by the expression analysis. *AtDGK1*, *AtDGK2*, *AtDGK3*, and *AtDGK5* were upregulated upon exposure to low temperature (4 °C) and contributed to the cold stress response in *Arabidopsis* [23,56]. Similarly, the expression of *TaDGK1A/B/D* and *TaDGK2D* genes increased significantly at 4 °C in wheat. Under salt stress, *MdDGK4* in apple and *PtDGK3/5* in poplar were induced in the plant salt response [19,22]. In the present study, *cis*-elements in the promoter of *AvDGK* genes were involved in phytohormone and stress responses, and plant growth and development. The results showed that MeJA responsiveness elements (TGACG motif and CGTCA motif) were present in almost all *AvDGK* genes, suggesting that *AvDGK* might be associated with MeJA signal transduction and involved in plant defensive responses against environmental stress [63]. Moreover, stress-related, *cis*-acting elements such as wound stress responsiveness, drought responsiveness, low-temperature responsiveness, anaerobic induction, defense, and stress responsiveness were also found in the promoters of *AvDGK* genes. Among them, anaerobic induction element (ARE) was commonly distributed, indicating that *AvDGK* might play an important role in *A. valvata* during low-oxygen (hypoxia) stress, which is usually caused by root waterlogging and submergence [64].

The gene function was further investigated by determining the expression patterns of *AvDGK* according to the available transcriptome data. Based on the transcriptome data, the expression levels of most *AvDGK* genes increased during the breaker fruit stage, suggesting that signal lipids such as DAG and PA are implicated by the ethylene signaling that is activated during fruit ripening [65,66]. It was reported that PA increased during tomato fruit pericarp ripening [67]. Moreover, the DGK genes identified in other plants have been reported to be significantly induced in response to salt stress, such as *PvDGKs* in the common bean [16], *AtDGK5* in *Arabidopsis* [28], *TaDGK2A/3A/5B/5A2* in wheat [18], and *GmDGKs* in soybean [20]. To estimate the response of *AvDGK* to salt stress, transcriptome data for *A. valvata* were downloaded and examined. The results showed that the expression levels of most *AvDGK* genes in the roots decreased, with the exception of *AvDGK13a/b*. PA synthesis in response to long-term salt stress mainly occurred through the hydrolysis of PLD, whereas a short-term salt stress might cause PA accumulation via the alternative PLC/DAG kinase pathway [68]. The downregulation of *AvDGK* genes under salt stress

might be a strategy for lipid remodeling, which could maintain the cell integrity and stability [69], as well as being helpful for energy conservation due to the use of ATP as an energy source by DGK to catalyze the conversion of DAG to PA.

Increasing evidence suggests that DGK and its product PA are involved in plant acclimation to waterlogging [28,29]. In *Arabidopsis*, the relative transcript levels of *AtDGK1* and *AtDGK5* were upregulated 10 min after submergence [29]. In our study, a qRT-PCR analysis was used to examine the relative expression levels of *AvDGK* genes after waterlogging treatment, which showed that the expression levels of *AvDGK12a*, *AvDGK12b*, and *AvDGK18b* were significantly induced under waterlogging stress. Previous studies reported that the levels of PA increased significantly in various plant species in response to submergence treatment [70,71], facilitating plant adaptations to hypoxia and improving plant tolerances to submergence [72]. Given that DGK synthesizes PA through the phosphorylation of DAG, expression upregulation of DGK was observed in *Arabidopsis* [29] and *A. valvata*. Moreover, *AvDGK12b* and *AvDGK18b* were induced rapidly, indicating their roles in the immediate response to short-term waterlogging stress, while *AvDGK12a* might be involved in regulating the long-term waterlogging stress response. We propose that the *AvDGK* gene family in the tetraploid *A. valvata*'s genome promoted PA synthesis and subsequent signal transduction under both short-term and long-term waterlogging stresses, which played a key role in enhancing the tolerance of kiwifruit to waterlogging stress.

5. Conclusions

In this study, a total of 18 *AvDGK* genes were identified and systematically analyzed in *A. valvata*. Based on multiple sequence alignment and a phylogenetic analysis, they were divided into three clusters. The motif and functional domains analysis further confirmed the classification and their phylogenetic relationships, and members within the same cluster had similar domain distributions, exon-intron structures, and conserved motif compositions. The collinearity analysis revealed that there were 29 duplicated gene pairs in *A. valvata*, and all had undergone purifying selection during evolution. Additionally, *cis*-elements in the promoter region were analyzed, indicating that the *cis*-elements within *AvDGK* genes are associated with multiple functions, including phytohormone signal transduction, the stress response, and plant growth and development. The expression levels of *AvDGK* genes including *AvDGK12a*, *AvDGK12b*, and *AvDGK18b* were significantly upregulated under waterlogging stress, suggesting that *AvDGKs* play an important role in the response to waterlogging stress. Thus, our findings provide a theoretical foundation for the further exploration of candidate genes to enhance kiwifruit's tolerance to waterlogging stress.

Supplementary Materials: The following supporting information can be downloaded at <https://www.mdpi.com/article/10.3390/horticulturae10040310/s1>: Figure S1: An amino acid similarity analysis of the *AvDGK* proteins with DGK from *A. thaliana*. Figure S2: The secondary structure of the *AvDGKs*. Figure S3: Sequence logos for 10 conserved motifs identified in the *AvDGKs*. Figure S4: Numbers of exon-intron pairs in the *AvDGK* gene family. Table S1: The primer pairs used in the RT-qPCR analysis. Table S2: Chromosomal location of the *AvDGK* genes. Table S3: The secondary structure analysis of the *AvDGK* proteins. Table S4: Duplication events identified in *AvDGKs*.

Author Contributions: Conceptualization, M.Z. and C.L.; methodology, M.Z.; software, F.W. and B.Q.; validation, M.Z., C.L. and F.W.; formal analysis, J.L.; investigation, M.Z., J.G. and K.Y.; resources, S.L.; data curation, Q.M.; writing—original draft preparation, M.Z.; writing—review and editing, C.L.; visualization, C.L.; supervision, H.G.; project administration, C.L.; funding acquisition, C.L. All authors have read and agreed to the published version of the manuscript.

Funding: This work was supported by the National Natural Science Foundation of China (32060643, 32060666, 32160084), Guangxi Science and Technology Program (Guike AD23026228), Guilin Innovation Platform and Talent Plan (20220125-7), the Fundamental Research Fund of Guangxi Institute of Botany (23008), Guangxi Science and Technology Major Project (Guike AA23023008), Earmarked Fund for China Agriculture Research System (nycytxgxcxtd-2023-13-01), Doctoral Research Funding from Shangluo University (17SKY016), and Natural Science Foundation of Hunan Province (2023JJ30488).

Data Availability Statement: Data are contained within the article and Supplementary Materials.

Conflicts of Interest: The authors declare no conflicts of interest.

References

1. Yao, S.; Kim, S.; Li, J.; Tang, S.; Wang, X. Phosphatidic acid signaling and function in nuclei. *Prog. Lipid Res.* **2024**, *93*, 101267. [[CrossRef](#)] [[PubMed](#)]
2. Kong, L.; Ma, X.; Zhang, C.; Kim, S.; Li, B.; Xie, Y.; Yeo, I.; Thapa, H.; Chen, S.; Devarenne, T.P.; et al. Dual phosphorylation of DGK5-mediated PA burst regulates ROS in plant immunity. *Cell* **2024**, *187*, 609–623.e21. [[CrossRef](#)] [[PubMed](#)]
3. Ali, U.; Lu, S.; Fadlalla, T.; Iqbal, S.; Yue, H.; Yang, B.; Hong, Y.; Wang, X.; Guo, L. The functions of phospholipases and their hydrolysis products in plant growth, development and stress responses. *Prog. Lipid Res.* **2022**, *86*, 101158. [[CrossRef](#)] [[PubMed](#)]
4. Hong, Y.; Zhao, J.; Guo, L.; Kim, S.; Deng, X.; Wang, G.; Zhang, G.; Li, M.; Wang, X. Plant phospholipases D and C and their diverse functions in stress responses. *Prog. Lipid Res.* **2016**, *62*, 55–74. [[CrossRef](#)] [[PubMed](#)]
5. Kim, S.; Wang, X. Phosphatidic acid: An emerging versatile class of cellular mediators. *Essays Biochem.* **2020**, *64*, 533–546. [[CrossRef](#)] [[PubMed](#)]
6. Testerink, C.; Munnik, T. Phosphatidic acid: A multifunctional stress signaling lipid in plants. *Trends Plant Sci.* **2005**, *10*, 368–375. [[CrossRef](#)] [[PubMed](#)]
7. Fan, B.; Liao, K.; Wang, L.; Shi, L.; Zhang, Y.; Xu, L.; Zhou, Y.; Li, J.; Chen, Y.; Chen, Q.; et al. Calcium-dependent activation of CPK12 facilitates its cytoplasm-to-nucleus translocation to potentiate plant hypoxia sensing by phosphorylating ERF-VII transcription factors. *Mol. Plant* **2023**, *16*, 979–998. [[CrossRef](#)] [[PubMed](#)]
8. Lindberg, S.; Premkumar, A.; Rasmussen, U.; Schulz, A.; Lager, I. Phospholipases AtPLD ζ 1 and AtPLD ζ 2 function differently in hypoxia. *Physiol. Plant.* **2018**, *162*, 98–108. [[CrossRef](#)] [[PubMed](#)]
9. Kolesnikov, Y.; Kretynin, S.; Bukhonska, Y.; Pokotylo, I.; Ruelland, E.; Martinec, J.; Kravets, V. Phosphatidic acid in plant hormonal signaling: From target proteins to membrane conformations. *Int. J. Mol. Sci.* **2022**, *23*, 3227. [[CrossRef](#)] [[PubMed](#)]
10. Park, J.; Gu, Y.; Lee, Y.; Yang, Z.; Lee, Y. Phosphatidic acid induces leaf cell death in Arabidopsis by activating the rho-related small G protein GTPase-mediated pathway of reactive oxygen species generation. *Plant Physiol.* **2004**, *134*, 129–136. [[CrossRef](#)]
11. Scholz, P.; Pejchar, P.; Fernkorn, M.; Škrabálková, E.; Pleskot, R.; Blerch, K.; Munnik, T.; Potocký, M.; Ischebeck, T. DIA-CYLGLYCEROL KINASE 5 regulates polar tip growth of tobacco pollen tubes. *New Phytol.* **2022**, *233*, 2185–2202. [[CrossRef](#)] [[PubMed](#)]
12. Kue Foka, I.C.; Keteouli, T.; Zhou, Y.; Li, X.; Wang, F.; Li, H. The emerging roles of diacylglycerol kinase (DGK) in plant stress tolerance, growth, and development. *Agronomy* **2020**, *10*, 1375. [[CrossRef](#)]
13. Escobar Sepúlveda, H.F.; Trejo Téllez, L.I.; Pérez Rodríguez, P.; Hidalgo Contreras, J.V.; Gómez Merino, F.C. Diacylglycerol kinases are widespread in higher plants and display inducible gene expression in response to beneficial elements, metal, and metalloids ions. *Front. Plant Sci.* **2017**, *8*, 227478. [[CrossRef](#)] [[PubMed](#)]
14. Arisz, S.A.; Testerink, C.; Munnik, T. Plant PA signaling via diacylglycerol kinase. *Biochim. Biophys. Acta* **2009**, *1791*, 869–875. [[CrossRef](#)] [[PubMed](#)]
15. Ge, H.; Chen, C.; Jing, W.; Zhang, Q.; Wang, H.; Wang, R.; Zhang, W. The rice diacylglycerol kinase family: Functional analysis using transient RNA interference. *Front. Plant Sci.* **2012**, *3*, 21372. [[CrossRef](#)] [[PubMed](#)]
16. Yeken, M.Z.; Özer, G.; Çiftçi, V. Genome-wide identification and expression analysis of DGK (diacylglycerol kinase) genes in common bean. *J. Plant Growth Regul.* **2023**, *42*, 2558–2569. [[CrossRef](#)]
17. Tang, F.; Xiao, Z.; Sun, F.; Shen, S.; Chen, S.; Chen, R.; Zhu, M.; Zhang, Q.; Du, H.; Lu, K.; et al. Genome-wide identification and comparative analysis of diacylglycerol kinase (DGK) gene family and their expression profiling in *Brassica napus* under abiotic stress. *BMC Plant Biol.* **2020**, *20*, 473. [[CrossRef](#)] [[PubMed](#)]
18. Jia, X.; Si, X.; Jia, Y.; Zhang, H.; Tian, S.; Li, W.; Zhang, K.; Pan, Y. Genomic profiling and expression analysis of the diacylglycerol kinase gene family in heterologous hexaploid wheat. *PeerJ* **2021**, *9*, e12480. [[CrossRef](#)] [[PubMed](#)]
19. Li, Y.; Tan, Y.; Shao, Y.; Li, M.; Ma, F. Comprehensive genomic analysis and expression profiling of diacylglycerol kinase gene family in *Malus prunifolia* (Willd.) Borkh. *Gene* **2015**, *561*, 225–234. [[CrossRef](#)] [[PubMed](#)]
20. Carther, K.F.I.; Keteouli, T.; Ye, N.; Yang, Y.H.; Wang, N.; Dong, Y.Y.; Yao, N.; Liu, X.M.; Liu, W.C.; Li, X.W.; et al. Comprehensive genomic analysis and expression profiling of diacylglycerol kinase (DGK) gene family in soybean (*Glycine max*) under abiotic stresses. *Int. J. Mol. Sci.* **2019**, *20*, 1361. [[CrossRef](#)] [[PubMed](#)]
21. Gu, Y.; Zhao, C.; He, L.; Yan, B.; Dong, J.; Li, Z.; Yang, K.; Xu, J. Genome-wide identification and abiotic stress responses of DGK gene family in maize. *J. Plant Biochem. Biotechnol.* **2018**, *27*, 156–166. [[CrossRef](#)]
22. Wang, H.; Yan, Z.; Yang, M.; Gu, L. Genome-wide identification and characterization of the diacylglycerol kinase (DGK) gene family in *Populus trichocarpa*. *Physiol. Mol. Plant Pathol.* **2023**, *127*, 102121. [[CrossRef](#)]
23. Gómez Merino, F.C.; Brearley, C.A.; Ornatowska, M.; Abdel Haliem, M.E.F.; Zantor, M.I.; Mueller Roeber, B. AtDGK2, a novel diacylglycerol kinase from *Arabidopsis thaliana*, phosphorylates 1-stearoyl-2-arachidonoyl-sn-glycerol and 1,2-dioleoyl-sn-glycerol and exhibits cold-inducible gene expression. *J. Biol. Chem.* **2004**, *279*, 8230–8241. [[CrossRef](#)] [[PubMed](#)]

24. Vaultier, M.N.; Cantrel, C.; Guerbette, F.; Boutté, Y.; Vergnolle, C.; Çiçek, D.; Bolte, S.; Zachowski, A.; Ruelland, E. The hydrophobic segment of *Arabidopsis thaliana* cluster I diacylglycerol kinases is sufficient to target the proteins to cell membranes. *FEBS Lett.* **2008**, *582*, 1743–1748. [[CrossRef](#)] [[PubMed](#)]
25. Snedden, W.A.; Blumwald, E. Alternative splicing of a novel diacylglycerol kinase in tomato leads to a calmodulin-binding isoform. *Plant J.* **2000**, *24*, 317–326. [[CrossRef](#)]
26. Gómez Merino, F.C.; Arana Ceballos, F.A.; Trejo Téllez, L.I.; Skirycz, A.; Brearley, C.A.; Dörmann, P.; Mueller Roeber, B. *Arabidopsis* AtDGK7, the smallest member of plant diacylglycerol kinases (DGKs), displays unique biochemical features and saturates at low substrate concentration. *J. Biol. Chem.* **2005**, *280*, 34888–34899. [[CrossRef](#)]
27. Yuan, S.; Kim, S.; Deng, X.; Hong, Y.; Wang, X. Diacylglycerol kinase and associated lipid mediators modulate rice root architecture. *New Phytol.* **2019**, *223*, 261–276. [[CrossRef](#)] [[PubMed](#)]
28. Li, J.; Yao, S.; Kim, S.; Wang, X. Lipid phosphorylation by a diacylglycerol kinase suppresses ABA biosynthesis to regulate plant stress responses. *Mol. Plant* **2024**, *17*, 342–358. [[CrossRef](#)]
29. Zhou, Y.; Zhou, D.; Yu, W.; Shi, L.; Zhang, Y.; Lai, Y.; Huang, L.; Qi, H.; Chen, Q.; Yao, N.; et al. Phosphatidic acid modulates MPK3- and MPK6-mediated hypoxia signaling in *Arabidopsis*. *Plant Cell* **2021**, *34*, 889–909. [[CrossRef](#)]
30. Huo, L.; Wang, H.; Wang, Q.; Gao, Y.; Xu, K.; Sun, X. Exogenous treatment with melatonin enhances waterlogging tolerance of kiwifruit plants. *Front. Plant Sci.* **2022**, *13*, 1081787. [[CrossRef](#)]
31. Wurms, K.V.; Reglinski, T.; Buissink, P.; Ah Chee, A.; Fehlmann, C.; McDonald, S.; Cooney, J.; Jensen, D.; Hedderley, D.; McKenzie, C.; et al. Effects of drought and flooding on phytohormones and abscisic acid gene expression in Kiwifruit. *Int. J. Mol. Sci.* **2023**, *24*, 7580. [[CrossRef](#)]
32. Huang, H. Systematics and genetic variation of *Actinidia*. In *Kiwifruit*; Academic Press: San Diego, CA, USA, 2016; Chapter 1, pp. 9–44. [[CrossRef](#)]
33. Ferguson, A.R.; Huang, H. Genetic resources of Kiwifruit: Domestication and breeding. In *Horticultural Reviews*; John Wiley & Sons, Inc.: Hoboken, NJ, USA, 2007; Chapter 1, pp. 1–121. [[CrossRef](#)]
34. Li, X.; Li, J.; Soejarto, D.D. Advances in the study of the systematics of *Actinidia* Lindley. *Front. Biol. China* **2009**, *4*, 55–61. [[CrossRef](#)]
35. Gao, M.; Gai, C.; Li, X.; Feng, X.; Lai, R.; Song, Y.; Zeng, R.; Chen, D.; Chen, Y. Waterlogging tolerance of *Actinidia valvata* Dunn is associated with high activities of pyruvate decarboxylase, alcohol dehydrogenase and antioxidant enzymes. *Plants* **2023**, *12*, 2872. [[CrossRef](#)]
36. Bai, D.; Li, Z.; Hu, C.; Zhang, Y.; Muhammad, A.; Zhong, Y.; Fang, J. Transcriptome-wide identification and expression analysis of *ERF* family genes in *Actinidia valvata* during waterlogging stress. *Sci. Hort.* **2021**, *281*, 109994. [[CrossRef](#)]
37. Li, Z.; Bai, D.; Zhong, Y.; Abid, M.; Qi, X.; Hu, C.; Fang, J. Physiological responses of two contrasting Kiwifruit (*Actinidia* spp.) rootstocks against waterlogging stress. *Plants* **2021**, *10*, 2586. [[CrossRef](#)]
38. Bai, D.; Zhong, Y.; Gu, S.; Qi, X.; Sun, L.; Lin, M.; Wang, R.; Li, Y.; Hu, C.; Fang, J. AvERF73 positively regulates waterlogging tolerance in kiwifruit by participating in hypoxia response and mevalonate pathway. *Hortic. Plant J.* **2024**. *in press*. [[CrossRef](#)]
39. Lamesch, P.; Berardini, T.Z.; Li, D.; Swarbreck, D.; Wilks, C.; Sasidharan, R.; Muller, R.; Dreher, K.; Alexander, D.L.; Garcia-Hernandez, M.; et al. The *Arabidopsis* Information Resource (TAIR): Improved gene annotation and new tools. *Nucleic Acids Res.* **2011**, *40*, D1202–D1210. [[CrossRef](#)]
40. Mistry, J.; Chuguransky, S.; Williams, L.; Qureshi, M.; Salazar, G.A.; Sonnhammer, E.L.L.; Tosatto, S.C.E.; Paladin, L.; Raj, S.; Richardson, L.J.; et al. Pfam: The protein families database in 2021. *Nucleic Acids Res.* **2020**, *49*, D412–D419. [[CrossRef](#)]
41. Potter, S.C.; Luciani, A.; Eddy, S.R.; Park, Y.; Lopez, R.; Finn, R.D. HMMER web server: 2018 update. *Nucleic Acids Res.* **2018**, *46*, W200–W204. [[CrossRef](#)] [[PubMed](#)]
42. Chou, K.; Shen, H. Plant-mPLOC: A top-down strategy to augment the power for predicting plant protein subcellular localization. *PLoS ONE* **2010**, *5*, e11335. [[CrossRef](#)] [[PubMed](#)]
43. Geourjon, C.; Deléage, G. SOPMA: Significant improvements in protein secondary structure prediction by consensus prediction from multiple alignments. *Bioinformatics* **1995**, *11*, 681–684. [[CrossRef](#)] [[PubMed](#)]
44. Kelley, L.A.; Mezulis, S.; Yates, C.M.; Wass, M.N.; Sternberg, M.J.E. The Phyre2 web portal for protein modeling, prediction and analysis. *Nat. Protoc.* **2015**, *10*, 845–858. [[CrossRef](#)]
45. Liu, W.; Xie, Y.; Ma, J.; Luo, X.; Nie, P.; Zuo, Z.; Lahrmann, U.; Zhao, Q.; Zheng, Y.; Zhao, Y.; et al. IBS: An illustrator for the presentation and visualization of biological sequences. *Bioinformatics* **2015**, *31*, 3359–3361. [[CrossRef](#)] [[PubMed](#)]
46. Goodstein, D.M.; Shu, S.; Howson, R.; Neupane, R.; Hayes, R.D.; Fazo, J.; Mitros, T.; Dirks, W.; Hellsten, U.; Putnam, N.; et al. Phytozome: A comparative platform for green plant genomics. *Nucleic Acids Res.* **2011**, *40*, D1178–D1186. [[CrossRef](#)] [[PubMed](#)]
47. Letunic, I.; Bork, P. Interactive Tree Of Life (iTOL) v5: An online tool for phylogenetic tree display and annotation. *Nucleic Acids Res.* **2021**, *49*, W293–W296. [[CrossRef](#)] [[PubMed](#)]
48. Bailey, T.L.; Johnson, J.; Grant, C.E.; Noble, W.S. The MEME Suite. *Nucleic Acids Res.* **2015**, *43*, W39–W49. [[CrossRef](#)] [[PubMed](#)]
49. Chen, C.; Wu, Y.; Li, J.; Wang, X.; Zeng, Z.; Xu, J.; Liu, Y.; Feng, J.; Chen, H.; He, Y.; et al. TBtools-II: A “one for all, all for one” bioinformatics platform for biological big-data mining. *Mol. Plant* **2023**, *16*, 1733–1742. [[CrossRef](#)]
50. Chao, J.; Li, Z.; Sun, Y.; Aluko, O.O.; Wu, X.; Wang, Q.; Liu, G. MG2C: A user-friendly online tool for drawing genetic maps. *Mol. Hort.* **2021**, *1*, 16. [[CrossRef](#)]
51. Wang, Y.; Tang, H.; DeBarry, J.D.; Tan, X.; Li, J.; Wang, X.; Lee, T.-h.; Jin, H.; Marler, B.; Guo, H.; et al. MCSanX: A toolkit for detection and evolutionary analysis of gene synteny and collinearity. *Nucleic Acids Res.* **2012**, *40*, e49. [[CrossRef](#)]

52. Zhang, Z.; Li, J.; Zhao, X.Q.; Wang, J.; Wong, G.K.; Yu, J. KaKs_Calculator: Calculating Ka and Ks through model selection and model averaging. *Genom. Proteom. Bioinform.* **2006**, *4*, 259–263. [[CrossRef](#)]
53. Lescot, M.; Déhais, P.; Thijs, G.; Marchal, K.; Moreau, Y.; Van de Peer, Y.; Rouzé, P.; Rombauts, S. PlantCARE, a database of plant cis-acting regulatory elements and a portal to tools for in silico analysis of promoter sequences. *Nucleic Acids Res.* **2002**, *30*, 325–327. [[CrossRef](#)] [[PubMed](#)]
54. Hou, Y.; Fan, C.; Sun, J.; Chang, Y.; Lu, J.; Sun, J.; Wang, C.; Liu, J. Genome-wide Identification, evolution, and expression analysis of the TCP gene family in rose (*Rosa chinensis* Jacq.). *Horticulturae* **2022**, *8*, 961. [[CrossRef](#)]
55. Livak, K.J.; Schmittgen, T.D. Analysis of relative gene expression data using real-time quantitative PCR and the $2^{-\Delta\Delta CT}$ method. *Methods* **2001**, *25*, 402–408. [[CrossRef](#)] [[PubMed](#)]
56. Arisz, S.A.; van Wijk, R.v.; Roels, W.; Zhu, J.; Haring, M.A.; Munnik, T. Rapid phosphatidic acid accumulation in response to low temperature stress in Arabidopsis is generated through diacylglycerol kinase. *Front. Plant Sci.* **2013**, *4*, 20590. [[CrossRef](#)]
57. Shen, L.; Zhuang, B.; Wu, Q.; Zhang, H.; Nie, J.; Jing, W.; Yang, L.; Zhang, W. Phosphatidic acid promotes the activation and plasma membrane localization of MKK7 and MKK9 in response to salt stress. *Plant Sci.* **2019**, *287*, 110190. [[CrossRef](#)] [[PubMed](#)]
58. Gao, Y.; Jiang, Z.; Shi, M.; Zhou, Y.; Huo, L.; Li, X.; Xu, K. Comparative transcriptome provides insight into responding mechanism of waterlogging stress in *Actinidia valvata* Dunn. *Gene* **2022**, *845*, 146843. [[CrossRef](#)] [[PubMed](#)]
59. Li, Z.; Zhong, Y.; Bai, D.; Lin, M.; Qi, X.; Fang, J. Comparative analysis of physiological traits of three *Actinidia valvata* Dunn genotypes during waterlogging and post-waterlogging recovery. *Hortic. Environ. Biotechnol.* **2020**, *61*, 825–836. [[CrossRef](#)]
60. Li, Z.; Bai, D.; Zhong, Y.; Lin, M.; Sun, L.; Qi, X.; Hu, C.; Fang, J. Full-Length transcriptome and RNA-Seq analyses reveal the mechanisms underlying waterlogging tolerance in Kiwifruit (*Actinidia valvata*). *Int. J. Mol. Sci.* **2022**, *23*, 3237. [[CrossRef](#)] [[PubMed](#)]
61. Lynch, M.; O’Hely, M.; Walsh, B.; Force, A. The probability of preservation of a newly arisen gene duplicate. *Genetics* **2001**, *159*, 1789–1804. [[CrossRef](#)]
62. Rogozin, I.B.; Wolf, Y.I.; Sorokin, A.V.; Mirkin, B.G.; Koonin, E.V. Remarkable interkingdom conservation of intron positions and massive, lineage-specific intron loss and gain in eukaryotic evolution. *Curr. Biol.* **2003**, *13*, 1512–1517. [[CrossRef](#)] [[PubMed](#)]
63. Santino, A.; Taurino, M.; De Domenico, S.; Bonsegna, S.; Poltronieri, P.; Pastor, V.; Flors, V. Jasmonate signaling in plant development and defense response to multiple (a)biotic stresses. *Plant Cell Rep.* **2013**, *32*, 1085–1098. [[CrossRef](#)] [[PubMed](#)]
64. León, J.; Castillo, M.C.; Gayubas, B. The hypoxia–reoxygenation stress in plants. *J. Exp. Bot.* **2020**, *72*, 5841–5856. [[CrossRef](#)] [[PubMed](#)]
65. Chen, T.; Qin, G.; Tian, S. Regulatory network of fruit ripening: Current understanding and future challenges. *New Phytol.* **2020**, *228*, 1219–1226. [[CrossRef](#)] [[PubMed](#)]
66. Bhardwaj, S.; Verma, T.; Kapoor, D. Ethylene and regulation of metabolites in plants. In *Ethylene in Plant Biology*; John Wiley & Sons, Inc.: Hoboken, NJ, USA, 2022; Chapter 3, pp. 32–48. [[CrossRef](#)]
67. Whitaker, B.D.; Smith, D.L.; Green, K.C. Characterization of a phospholipase D α cDNA from tomato fruit. *Biochem. Soc. Trans.* **2000**, *28*, 819–821. [[CrossRef](#)] [[PubMed](#)]
68. Guo, Q.; Liu, L.; Barkla, B.J. Membrane lipid remodeling in response to salinity. *Int. J. Mol. Sci.* **2019**, *20*, 4264. [[CrossRef](#)] [[PubMed](#)]
69. Ge, S.; Liu, D.; Chu, M.; Liu, X.; Wei, Y.; Che, X.; Zhu, L.; He, L.; Xu, J. Dynamic and adaptive membrane lipid remodeling in leaves of sorghum under salt stress. *Crop J.* **2022**, *10*, 1557–1569. [[CrossRef](#)]
70. Xu, L.; Pan, R.; Zhou, M.; Xu, Y.; Zhang, W. Lipid remodelling plays an important role in wheat (*Triticum aestivum*) hypoxia stress. *Funct. Plant Biol.* **2020**, *47*, 58–66. [[CrossRef](#)] [[PubMed](#)]
71. Wang, M.; Shen, Y.; Tao, F.; Yang, S.; Li, W. Submergence induced changes of molecular species in membrane lipids in *Arabidopsis thaliana*. *Plant Divers.* **2016**, *38*, 156–162. [[CrossRef](#)]
72. Xie, L.; Zhou, Y.; Chen, Q.; Xiao, S. New insights into the role of lipids in plant hypoxia responses. *Prog. Lipid Res.* **2021**, *81*, 101072. [[CrossRef](#)] [[PubMed](#)]

Disclaimer/Publisher’s Note: The statements, opinions and data contained in all publications are solely those of the individual author(s) and contributor(s) and not of MDPI and/or the editor(s). MDPI and/or the editor(s) disclaim responsibility for any injury to people or property resulting from any ideas, methods, instructions or products referred to in the content.